Multi-wavelength immunoassays using surface plasmon-coupled emission

Evgenia Matveeva, Joanna Malicka, Ignacy Gryczynski, Zygmunt Gryczynski, and Joseph R. Lakowicz*

Department of Biochemistry and Molecular Biology, Center for Fluorescence Spectroscopy, University of Maryland at Baltimore, 725 West Lombard Street, Baltimore, MD 21201, USA

Abstract

We describe a new method for multi-wavelength immunoassays using surface plasmon-coupled emission (SPCE). This phenomenon is coupling of excited fluorophores with a nearby thin metal film, in our case silver, resulting in strongly directional emission into the underlying glass substrate. The angle at which the radiation propagate through the prism depends on the surface plasmon angle for the relevant wavelength. These angles depend on emission wavelength, allowing measurement of multiple analytes using multiple emission wavelengths. We demonstrated this possibility using antibodies labeled with either Rhodamine Red-X or AlexaFluor 647. These antibodies were directed against an antigen protein bound to the silver surface. The emission from each labeled antibody occurred at a different angle on the glass prism, allowing independent measurement of surface binding of each antibody. This method of SPCE immunoassays can be readily extended to 4 or more wavelengths.
© 2003 Elsevier Inc. All rights reserved.

Fluorescence immunoassays are widely used in the biosciences [1–3]. Such immunoassays can be based on anisotropy [4,5], energy transfer [6,7], or time-gating [8,9]. Regardless of the chosen observable quality, the immunoassays are invariably based on the free-space emission of the probes. By free-space (FS) emission we mean the nearly isotropic emission of fluorophores into homogeneous transparent media.

In several recent papers we described a new approach to fluorescence detection in which the FS emission is altered by near-field interactions with a metallic surface [10,11]. The changes in emission can be favorable, including changes in quantum yield, photostability, and energy transfer. These effects rely upon the interactions of fluorophores with sub-wavelength size silver particles.

More recently we described a different near field interaction which occurs between excited fluorophores and a thin metal film, typically 50 nm thick silver or gold [12–15]. We found coupling of the excited fluorophores with surface plasmons in the metal resulted in highly directional emission and/or transfer of energy through the metal into the underlying glass substrate. We refer to this phenomenon as surface plasmon-coupled emission (SPCE). The angles for SPCE were shown to depend on the emission wavelength.
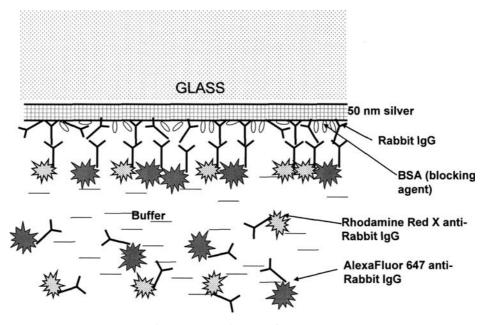
In the present report we describe the use of SPCE, and its angular dependence on wavelength, to develop a two wavelength immunoassay with two different labeled antibodies (Scheme 1). The SPCE of each detected antibody, which occurred at a different wavelength, appeared at different angles in the glass prism. This method can be readily extended to more analytes using fluorophores emitting at different wavelengths. SPCE immunoassays also have the favorable properties of background suppression due to the excitation and collection of emission being localized near the metal surface. We expect multiplexed SPCE immunoassays to become widely used in medical testing.

Materials and methods

Reagents. Rabbit IgG (11.2 mg/mL) was from Sigma. Rhodamine Red-X-antiRabbit IgG (produced in goat, 2 mg/mL,

---

* Corresponding author. Fax: 1-410-706-8408.
E-mail address: lakowicz@cfs.umbi.umd.edu (J.R. Lakowicz).
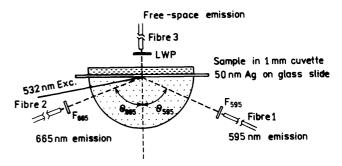
Scheme 1. Two-color SPCE immunoassay.

dye/protein = 3.8 mol/mol) and AlexaFluor647-antiRabbit IgG (produced in goat, 2 mg/mL, dye/protein = 4.5 mol/mol) conjugates were from Molecular Probes. Buffer components and salts (such as bovine serum albumin, glucose, and sucrose) were from Sigma–Aldrich.

Coating slides with IgG. Standard glass microscope slides (3 × 1 in., 1 mm thick; Corning) were vapor deposited with a continuous 50 nm thick silver layer by EMF (Ithaca, NY). Slides were non-covalently coated with rabbit IgG: 1.6 mL coating solution of IgG (50 μg/mL IgG in Na-phosphate buffer, 50 mM, pH 7.4) was added to the slide, and slide was incubated 3.5 h at room temperature in a humid chamber. Slides were then rinsed with water, washing solution (0.05% Tween 20 in water), and water. Blocking was performed by adding 2.0 mL of blocking buffer (1% bovine serum albumin (BSA), 1% sucrose, 0.05% NaN$_3$, 0.05% Tween 20 in 50 mM Tris–HCl buffer, pH 7.4) and incubation overnight at +4 °C in humid chamber. The slides were rinsed with water, washing solution (0.05% Tween 20 in water), and water, covered with blocking buffer and stored at +4 °C until use.

End-point binding experiment. Two dye-labeled conjugates, Rhodamine Red-X-antiRabbit IgG (RhX-Ab) and AlexaFluor647-antiRabbit IgG (Alexa-Ab) were mixed in blocking solution: 20 μL of each stock conjugate solution was added to 4 mL of blocking solution. This mixture was added to the slides (1.5 mL per slide), and slides were incubated at 37 °C in a humid chamber for 1 h. Slides then were rinsed with water, washing solution (0.05% Tween 20 in water), and water. A 1 mm thick cuvette was mounted on the metallic side of the slide. About 0.4 mL of the blocking buffer was added inside the cuvette, and fluorescence measurements were performed at two different optical configurations (Kretschmann and reverse Kretschmann).

Kinetic binding experiment. A 1 mm thick cuvette was mounted on the metallic side of the slide (coated with rabbit IgG as described above). About 0.4 mL of the mixture of two dye-labeled conjugates Rhodamine Red-X-antiRabbit IgG and AlexaFluor647-antiRabbit IgG (prepared as described above) was added into the cuvette using a needle. Kinetics was immediately monitored at room temperature (17 °C) using the configuration shown in Scheme 2.

Spectroscopic measurements. Fluorescence measurements on microscope slides were performed using index-matching fluid to attach the slide to a hemicylindrical prism made of BK7 glass and positioned on a precise rotatory stage equipped with the fiber optics mount on a 15 cm long arm [13]. This configuration allowed fluorescence observation at any angle relative to the incident angle. The output of the

Scheme 2. Experimental configuration for the two-color SPCE assay using surface plasmon (Kretschmann) excitation. Fibres F$_1$ and F$_2$ collect SPCE at 595 and 665 nm, respectively. Fibre F$_3$ observes the free-space emission.

fiber was connected to an Ocean Optics SD2000 spectrofluorometer for emission spectra. The excitation at 532 nm was from a solid-state laser (maximal output power 30 mW). The kinetic measurements were done with simultaneous observation through three fibers pointing to three independent detectors.

Theory

The phenomenon of SPCE is closely related to surface plasmon resonance (SPR). The theory of surface plasmons has been described in details [16,17] as have its use to measure bioaffinity reactions [18,19]. Surface plasmons are excited when a metal surface is illuminated under specific conditions which allow wavevector matching at the sample metal interface. Surface plasmons cannot be excited from air by incident light. SPR occurs when light is incident on a metal through a higher refractive index medium such as glass. The surface plasmons are only excited at a specific angle of incident

(θ_{SP}), where the reflectivity decreases. At other angles of incidence (θ_I) the reflectivity of the metal is high.

The wavevector of the incident light in the prism is given by $k_p = 2\pi/\lambda = n_p k_0$, where λ is the wavelength in the prism, n_p is the refractive index of the prism, and k_0 is the wavevector in a vacuum or air. The in-plane x-component of the wavevector is given by

$$k_x = k_0 n_p \sin \theta_I, \tag{1}$$

where θ_I is measured from the normal axis (Scheme 2). SPR occurs when

$$k_{SP} = k_x = k_0 n_p \sin \theta_{SP}. \tag{2}$$

Calculation of the surface plasmon wavevector is somewhat complex. For a metal the dielectric constant is usually an imaginary number

$$\epsilon_m = \epsilon_r + i\epsilon_{im}, \tag{3}$$

where $i = \sqrt{-1}$ and the subscripts indicate the real (r) and imaginary (im) components. These constants are wavelength (frequency) dependent. Because the real part of ϵ_m is larger than the imaginary part the wavevector of a metal can usually be approximated by

$$k_{SP} = k_0 \left(\frac{\epsilon_r \epsilon_s}{\epsilon_r + \epsilon_s} \right)^{1/2}, \tag{4}$$

where ϵ_s is the effective dielectric constant of the sample near the silver surface. SPR only occurs for p-polarized incident light.

SPCE is similar to SPR in reverse. Instead of illumination through a prism, the metal feels near-field interactions with an excited fluorophore, resulting in creation of surface plasmons. These plasmons then radiate into the glass substrate at the surface plasmon angle for the emission wavelength (θ_F). The plasmons radiate at the plasmon angle because this is needed to match the wavevectors. The plasmons cannot radiate into the sample because the wavevectors cannot be matched. The angle θ_{SP} depends on wavelength because k_x depends on wavelength.

For SPCE the sample can be illuminated in two ways. The metal surface can be illuminated from the water side, the reverse Kretschmann (RK), which itself cannot create surface plasmons. The excited fluorophores near the metal can couple and create SPCE. Since the incident field does not undergo a resonance interaction with the metal the fluorophores are excited nearly equally across the sample. The device can also be illuminated through the prism, called the Kretschmann (KR) configuration (Scheme 2). When $\theta_I = \theta_{SP}$ there exists an evanescent field in the sample that extend out to about 200 nm above the metal. This evanescent field is enhanced about 40-fold by the resonance interaction [20]. Hence KR illumination results in selective excitation near the metal surface. The enhanced field can allow the incident intensity to be decrease while obtaining the same emission intensity, further reducing the background.

Results

The experimental configuration used for two-wavelength SPCE is shown in Scheme 2. The protein-coated silver surface is illuminated at the surface plasmon angle through the glass prism, which is called the Kretschmann (KR) configuration. The free-space emission is observed normal to the sample surface, on the side distal from the prism, using a filter and a fiber optic bundle. SPCE is observed on the prism side of the sample, at two different angles through appropriate long-pass filters for each labeled antibody. The sample can also be excited through the aqueous phase, which is called the reverse Kretschmann (RK) configuration.
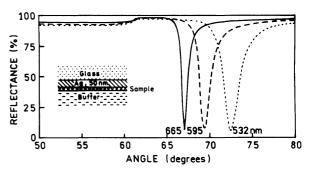

Fig. 1. Calculated reflectivity of a 50 nm silver film on BK7 glass ($n_p = 1.52$). The sample (protein layers) was assumed to be 15 nm thick ($n_s = 1.50$). The buffer thickness was taken as infinite with $n_w = 1.33$. For silver phase we used $\epsilon_m^{532} = -11.5 + 0.3i$, $\epsilon_m^{595} = -15.0 + 0.4i$, and $\epsilon_m^{665} = -21.0 + 0.6i$ [12].
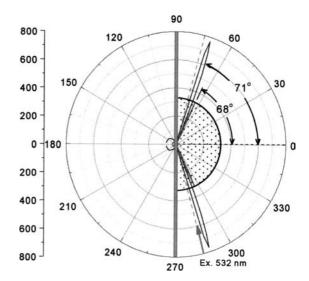

Fig. 2. Angle-dependent emission from a surface containing RhX-Ab and Alexa-Ab. Emission was measured at 595 or 665 nm. The sample was excited at 532 nm at 75° using the Kretschmann configuration.

In previous reports we found close agreement between the calculated reflectivity minima for the emission wavelength and the observed SPCE angles [12–14]. Hence we calculated the reflectivity expected for over the 50 nm thick silver films and our optical configuration (Fig. 1). The reflectivity curves can be calculated using either software available on the web [21] or commercial software [22] which we found to yield equivalent results. The reflectivity minima were found at 72.5° for 532 nm, and at 69° and 67° for 595 and 665 nm, respectively. Hence we expected to obtain excitation of surface plasmons with a 532 nm at incident angle of 72.5°, and to observe the RhX-Ab and Alexa-Ab emission at 69° and 67°, respectively.

We examined the angle-dependent emission intensity for an antigen (rabbit IgG) covered surface which was saturated with a mixture of RhX-Ab and Alexa-Ab (Fig. 2). The emission from both labeled antibodies was strongly directional at different angles on the prism. The emission from RhX-Ab peaked at 71°, and that from Alexa-Ab at 68°. It is important to recognize that SPCE does not require excitation of surface plasmons by the incident light. To demonstrate this fact we excited the sample through the aqueous phase (Fig. 3). Once again the emission from each labeled antibody was strongly directional in the prism at the surface plasmon angle for the emission wavelength. This result demonstrates that SPCE is due to an interaction of the excited fluorophores with the metal surface and does not depend on creation of surface plasmons by the incident light.

The angle-dependent intensities in Figs. 2 and 3 were collected through a emission filter to isolate the emission from each labeled antibody. However, these measurements did not resolve the emission spectra of each antibody. Fig. 4 shows emission spectra collected using observation angles of 71°, 69.5°, and 68°. At 71° the emission is almost completely due to RhX-Ab with an emission maximum of 595 nm. At 68° the emission is
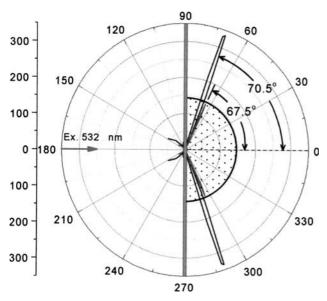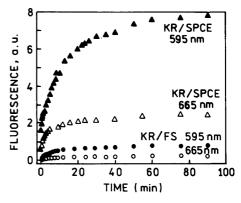

Fig. 3. Angle-dependent emission from surface-bound RhX-Ab and Alexa-Ab measured at 595 and 665 nm. The sample was excited at 532 nm using the RK configuration.

Fig. 5. Surface binding kinetics for the SPCE emission (▲, △) observed as shown in Scheme 2 and Fig. 2, at 71° for 595 nm and −68° for 665 nm. Free-space emission (●, ○).
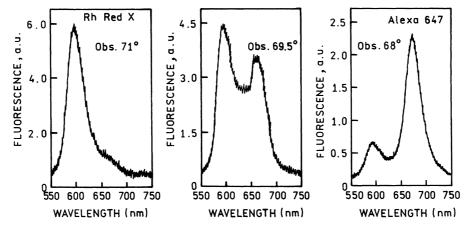

Fig. 4. Emission spectra from a surface containing RhX-Ab and Alexa-Ab measured at three observations angles, using the KR configuration.

due mostly to Alexa-Ab at 665 nm, with a residual component from RhX-Ab at 595 nm. At the intermediate angle of 69.5° the emission from both labeled antibodies is seen. These emission spectra show that the desired emission wavelength can be selected by adjustment of the observation angle.

We used SPCE at two observed angles to simultaneously measure the binding kinetics of both labeled antibodies (Fig. 5). The binding kinetics were similar even though the final intensities are different (▲, △). The binding was also measured using KR excitation and the free-space emission (●, ○). The intensities are over 10-fold higher for SPCE than for the free-space emission.

Discussion

We expect angle and wavelength-dependent SPCE to have numerous applications in sensing. The silver film serves multiple purposes. It amplifies the incident light [18], efficiently collects the emission, and provides separation of the wavelengths [12,13]. Detection could be accomplished with imaging or point detectors, to provide a simple yet sensitive device. The number of analytes can be increased by using fluorophores with emission wavelengths ranging from 450 to 800 nm. Still more analytes could be measured using semiconductor nanoparticles, which display narrow emission spectra [23,24]. We believe the angular dependence on wavelength can be increased using thin (50 nm) or thick (200 nm) metal gratings, which also display SPR with an additional dependence on the grating constant [25,26]. The use of the KR configuration localizes the excitation near the metal surface, but further localization is possible using multi-photon excitation [27,28]. The surface chemistry of silver and gold is well developed [29–33], and we recently observed SPCE using gold films [15]. SPCE is then an attractive approach for a wide range of sensing applications, which will often be based on novel device configurations.

Acknowledgments

References

[1] K. Van Dyke, R. Van Dyke (Eds.), Luminescence Immunoassay and Molecular Applications, CRC Press, Boca Raton, FL, 1990.

[2] I.A. Hemmila, Applications of Fluorescence in Immunoassays, John Wiley & Sons, New York, 1992.

[3] T. Vo-Dinh, M.J. Sepaniak, G.D. Griffin, J.P. Alarie, Immunosensors: principles and applications, Immunomethods 3 (1993) 85–92.

[4] M. Fiore, J. Mitchell, T. Doan, R. Nelson, G. Winter, C. Grandone, K. Zeng, R. Haraden, J. Smith, K. Harris, J. Leszczynski, D. Berry, S. Safford, G. Barnes, A. Scholnick, K. Ludington, The abbott IMx™ automated benchtop immunochemistry analyzer system, Clin. Chem. 34 (1988) 1726–1732.

[5] W.B. Dandliker, V.A. de Saussure, Fluorescence polarization in immunochemistry, Immunochemistry 7 (1970) 799–828.

[6] L.E. Morrison, Time-resolved detection of energy transfer: theory and application to immunoassays, Anal. Biochem. 174 (1988) 101–120.

[7] E.F. Ullman, M. Schwarzberg, K.E. Rubenstein, Fluorescent excitation transfer immunoassay: a general method for determination of antigens, J. Biol. Chem. 251 (14) (1976) 4172–4178.

[8] T. Lövgren, K. Pettersson, Time-resolved fluoroimmunoassay, advantages and limitations, in: K. Van Dyke, R. Van Dyke (Eds.), Luminescence Immunoassay and Molecular Applications, CRC Press, New York, 1990, pp. 234–250.

[9] E.P. Diamandis, Immunoassays with time-resolved fluorescence spectroscopy: principles and applications, Clin. Biochem. 21 (1988) 139–150.

[10] J.R. Lakowicz, Radiative decay engineering. Biophysical and biomedical applications, Anal. Biochem. 298 (2001) 1–24.

[11] J.R. Lakowicz, Y. Shen, S. D'Auria, J. Malicka, J. Fang, Z. Gryczynski, I. Gryczynski, Radiative decay engineering. 2. Effects of silver island films on fluorescence intensity, lifetimes and resonance energy transfer, Anal. Biochem. 301 (2002) 261–277.

[12] J.R. Lakowicz, Radiative decay engineering 3. Surface plasmon coupled directional emission, Anal. Biochem. (2003), in press.

[13] I. Gryczynski, J. Malicka, Z. Gryczynski, J.R. Lakowicz, Radiative decay engineering 4. Experimental studies of surface plasmon coupled directional emission, Anal. Biochem. (2003), in press.

[14] J. Malicka, I. Gryczynski, J. Fang, J. Kusba, J.R. Lakowicz, Photostability of Cy3 and Cy5 labeled DNA in the presence of metallic silver particles, J. Fluoresc. 12 (3/4) (2002) 439–447.

[15] I. Gryczynski, J. Malicka, Z. Gryczynski, J.R. Lakowicz, Surface plasmon-coupled emission using gold films (2003), submitted.

[16] H. Raether, Surface plasma oscillations and their applications, in: G. Hass, M.H. Francombe, R.W. Hoffman (Eds.), Physics of Thin Films, Advances in Research and Development, vol. 9, Academic Press, New York, 1977, pp. 145–261.

[17] H. Raether, Surface Plasmons on Smooth and Rough Surfaces and on Gratings, Springer-Verlag, New York, 1988, 136 pp.

[18] Z. Salamon, H.A. Macleod, G. Tollin, Surface plasmon resonance spectroscopy as a tool for investigating the biochemical and biophysical properties of membrane protein systems. I: theoretical principles, Biochim. Biophys. Acta 1331 (1997) 117–129.

[19] J. Melendez, R. Carr, D.U. Bartholomew, E. Kukanskis, J. Elkind, S. Yee, C. Furlong, R. Woodbury, A commercial solution for surface plasmon sensing, Sensors Actuators B 35–36 (1996) 212–216.

[20] T. Liebermann, W. Knoll, Surface-plasmon field-enhanced fluorescence spectroscopy, Colloids Surf. 171 (2000) 115–130.

[21] B.P. Nelson, A.G. Frutos, J.M. Brockman, R.M. Corn, Near-infrared surface plasmon resonance measurements of ultrathin films. 1. Angle shift and SPR imaging experiments, Anal. Chem. 71 (1999) 3928–3934.

[22] TF Calc., Software Spectra, Inc., Portland, Oregon.

[23] W.J. Parak, D. Gerlon, T. Pellegrino, D. Zanchet, C. Micheel, S.C. Williams, R. Boudreau, M. A Le Gros, C.A. Larabell, A.P. Alivisatos, Biological applications of colloidal nanocrystals, Nanotechnology 14 (2003) R15–R27.

[24] C.J. Murphy, J.L. Coffer, Quantum dots: a primer, Appl. Spectrosc. 56 (1) (2002) 16A–27A.

[25] S.C. Kitson, W.L. Barnes, J.R. Sambles, Photoluminescence from dye molecules on silver gratings, Opt. Commun. 122 (1996) 147–154.

[26] W. Knoll, M.R. Philpott, J.D. Swalen, Emission of light from Ag metal gratings coated with dye monolayer assemblies, J. Chem. Phys. 75 (10) (1981) 4795–4799.

[27] G.L. Duveneck, M.A. Bopp, M. Ehrat, L.P. Balet, M. Haiml, U. Keller, G. Marowsky, S. Soria, Two-photon fluorescence excitation of macroscopic areas on planar waveguides, Biosensors Bioelectron. 18 (2003) 503–510.

[28] H. Kano, S. Kawata, Two-photon-excited fluorescence enhanced by a surface plasmon, Opt. Lett. 21 (22) (1996) 1848–1850.

[29] G.K. Jennings, P.E. Laibinis, Underpotentially deposited metal layers of silver provide enhanced stability to self-assembled alkanethiol monolayers on gold, Langmuir 12 (1996) 6173–6175.

[30] S. Mandal, A. Gole, N. Lala, R. Gonnade, V. Ganvir, M. Sastry, Studies on the reversible aggregation of cysteine-capped colloidal silver particles interconnected via hydrogen bonds, Langmuir 17 (2001) 6262–6268.

[31] V. Salgueiriño-Maceira, F. Caruso, L.M. Liz-Marzán, Coated colloids with tailored optical properties, J. Phys. Chem. B 107 (2003) 10990–10994.

[32] C. Graf, D.L.J. Vossen, A. Imhof, A. van Blaaderen, A general method to coat colloidal particles with silica, Langmuir 19 (2003) 6693–6700.

[33] P.R. Selvakannan, S. Mandal, S. Phadtare, R. Pastricha, M. Sastry, Capping of gold nanoparticles by the amino acid lysine renders them water-dispersible, Langmuir 19 (2003) 3545–3549.